

***I* – Love – *C* relation for an anisotropic neutron star**H. C. Das ^{*}*Institute of Physics, Sachivalaya Marg, Bhubaneswar 751005, India and Homi Bhabha National Institute, Training School Complex, Anushakti Nagar, Mumbai 400094, India* (Received 31 August 2022; accepted 21 October 2022; published 16 November 2022)

One of the most common assumptions has been made that the pressure inside the star is isotropic in nature. However, the pressure is locally anisotropic in nature which is a more realistic case. In this study, we investigate certain properties of anisotropic neutron stars with the scalar pressure anisotropy model. Different perfect fluid conditions are tested within the star with the relativistic mean-field model equation of states (EOSs). The anisotropic neutron star properties such as mass (M), radius (R), compactness (C), Love number (k_2), dimensionless tidal deformability (Λ), and the moment of inertia (I) are calculated. The magnitude of the quantities as mentioned above increases (decreases) with the positive (negative) value of anisotropy except k_2 and Λ . The universal relation I – Love – C is calculated with almost 58 EOS spans from relativistic to nonrelativistic cases. We observed that the relations between them get weaker when we include anisotropy. With the help of the GW170817 tidal deformability limit and radii constraints from different approaches, we find that the anisotropic parameter is less than 1.0 if one uses the Bowers-Liang (BL) model. Using the universal relation and the tidal deformability bound given by the GW170817, we put a theoretical limit for the canonical radius, $R_{1.4} = 10.74^{+1.84}_{-1.36}$ km, and the moment of inertia, $I_{1.4} = 1.77^{+0.17}_{-0.09} \times 10^{45}$ g cm² with 90% confidence limit for isotropic stars. Similarly, for anisotropic stars with $\lambda_{BL} = 1.0$, the values are $R_{1.4} = 11.74^{+2.11}_{-1.54}$ km, $I_{1.4} = 2.40^{+0.17}_{-0.08} \times 10^{45}$ g cm² respectively.

DOI: [10.1103/PhysRevD.106.103518](https://doi.org/10.1103/PhysRevD.106.103518)**I. INTRODUCTION**

Exploration of the internal structure of compact stars such as neutron stars (NSs) is one of the most challenging problems because its study involves different areas of physics. Until now, we do not have a complete theoretical understanding of this object because it has a complex inner structure and strong gravity [1]. Besides this, we take another realistic phenomenon inside the compact objects termed pressure anisotropy. One of the most common assumptions in studying a neutron star's equilibrium structure is that its pressure is isotropic. However, the exact case is different due to some exotic process that happens inside it (for a review, see [2]). For example, very high magnetic field [3–10], pion condensation [11], phase transitions [12], relativistic nuclear interaction [13,14], crystallization of the core [15], superfluid core [16–18], etc. are the main causes of the anisotropy inside a star.

A diversity of anisotropic models in literature have been constructed for the matter with a perfect fluid. Mainly Bowers-Liang (BL) [19], Horvat *et al.* [20], and Cosenza *et al.* [21] models have been proposed. The BL model is based on the assumptions that (i) the anisotropy should vanish quadratically at the origin, (ii) the anisotropy should depend nonlinearly on radial pressure, and (iii) the

anisotropy is gravitationally induced. Horvat *et al.* proposed that anisotropy is due to the quasilocal equation as given in Ref. [20]. Different studies put the limit of anisotropic parameter, e.g., $-2 \leq \lambda_{BL} \leq +2$ for the BL model [22] and $-2 \leq \lambda_H \leq +2$ [23] for the Horvat model. In the present case, we take the BL model, which is explained in the following subsection.

Several studies explained the effects of anisotropic pressure on the macroscopic properties of the compact objects, such as its mass, radius, moment of inertia, tidal deformability, nonradial oscillation [22–40]. In general, it is observed that with increasing the magnitude of the anisotropy parameter, the magnitudes of macroscopic properties increase and vice versa. Contrary to mass and radius, the oscillation frequency of the anisotropic NS decreases [23]. In Ref. [26], it was suggested that the secondary component might be an anisotropic NS, contradicted in [32]. Deb *et al.* [27] have claimed that with increasing anisotropy, the star with a transverse magnetic field becomes more massive, increasing the star's size and vice versa for the radial field. Using the Skyrme model, Silva *et al.* [22] claimed that the observations of the binary pulsar might constrain the degree of anisotropy. Using GW170817 tidal deformability constraint, Biswas and Bose [35] observed that a certain equation of state (EOS) becomes viable if the star has enough anisotropy without the violation of causality. In Ref. [32], it has been

^{*}harish.d@iopb.res.in

observed that not only the BL model but the Horvat model is also well consistent with recent multimessenger constraints [32].

In this study, we calculate the NS properties for different degrees of anisotropy with the modern EOSs. Existing universal relations are explored between different anisotropic NS properties such as the moment of inertia (I), tidal deformability (Love), and compactness (C) ($I - \text{Love} - C$) by varying anisotropic parameters. Yagi and Yunes first obtained the universal relation for the $I - \text{Love} - Q$ (where Q is the quadrupole moment) for the slowly rotating and tidally deformed NS [41] and also for anisotropic NS [42]. Several studies have been dedicated to explaining the universal relations between different macroscopic properties of the compact objects [41–48]. This is because certain physical quantities are found to be interrelated with each other, and the relations are almost independent of the internal structure of the star. Therefore, the EOS insensitive relations are required to decode the information about others, which may not be observationally accessible.

Several studies put constraints on some properties of the NS, such as radius, the moment of inertia (MI), compactness, etc., using the observational data. Lattimer and Schutz constrain the EOSs by measuring MI in the double pulsars system [49]. Brew and Rezzolla [50] have explained some universal relations for the Keplerian star and also improved the universal relations given by Lattimer and Schutz. This study explains the universal relation $I - \text{Love} - C$ for the anisotropic NS. From those relations, we try to constrain the anisotropy parameter with the help of present observational data. Also, we put some theoretical limits on MI, compactness, and radius of both isotropic as well as anisotropic stars.

Exploration of compact star properties needs the EOS, which describes the internal mechanism and interactions between different particles present inside the star. The EOS is the relation between pressure and density, which includes all types of interactions occurring inside the star. For this, we use the relativistic mean-field (RMF) model [51–56], and the Skyrme-Hartree-Fock (SHF) model [57–60], which is non-relativistic in nature. The past few decades, both models played well in different areas of nuclear astrophysics [61–66]. In recent years, number of extended RMF (E-RMF) models have been put forth, and it has been discovered that the properties of various systems, including finite nuclei, nuclear matter, and neutron stars, are accurately replicated and consistent with experimental and observational evidence [66–69]. More than 200 parameter sets have been modeled by the different theoretical groups with either relativistic or nonrelativistic approaches. Among them, only a few EOSs have satisfied both nuclear matter properties and reproduced the latest massive NS mass, radius, and tidal deformability called the consistent model [55,60,70].

In this study, we choose RMF unified EOSs for $npe\mu$ matter which are BKA24, FSU2, FSUGarnet, G1, G2, G3, GL97, IOPB, IUFSU, IUFSU*, SINPA, SINPB, TM1 with

standard nonlinear interactions and higher-order couplings from Parmar *et al.* [71]. Other unified EOSs which are taken from Fortin *et al.* [72] are the hyperonic $npe\mu Y$ -matter variants BSR2Y, BSR6Y, GM1Y, NL3Y, NL3Yss, NL3 $\omega\rho$ Y, NL3 $\omega\rho$ Yss, DD2Y, and DDME2Y; the density-dependent linear models such as DD2, DDH δ , and DDME2, and the SHF $npe\mu$ -matter models BSk20, BSk21, BSk22, BSk23, BSk24, BSk25, BSk26, KDE0v1, Rs, SK255, SK272, SKa, SKb, SkI2, SkI3, SkI4, SkI5, SkI6, SkMP, SKOp, SLY230a, SLY2, SLY4, and SLY9. All the EOSs are able to reproduced the mass of the NS $\sim 2 M_{\odot}$. With these EOSs, we calculate the anisotropic star properties and calculate the $I - \text{Love} - C$ relations by varying anisotropy parameters. We use the value of G and c as equal to 1 in this calculation.

II. ANISOTROPIC CONFIGURATIONS

We consider a static and spherically symmetric equilibrium distribution of matter. The stress-energy tensor is defined as [73]

$$T_{\mu\nu} = (\mathcal{E} + P)u_{\mu}u_{\nu} + Pg_{\mu\nu}, \quad (1)$$

where \mathcal{E} and P are the energy density and pressure of the fluid. The u_{μ} is the four-velocity of the fluid respectively.

The anisotropy of the fluid means when the radial pressure (P_r) differs from the tangential pressure (P_t). The stress-energy tensor for the corresponding star is defined as [22,23,28]

$$T_{\mu\nu} = (\mathcal{E} + P_t)u_{\mu}u_{\nu} + (P_r - P_t)k_{\mu}k_{\nu} + P_t g_{\mu\nu}, \quad (2)$$

where k_{μ} is the unit radial vector ($k^{\mu}k_{\mu} = 1$) with $u^{\mu}k_{\mu} = 0$.

For a spherically symmetric, nonrotating NS, the metric is defined as

$$ds^2 = e^{\nu} dt^2 - e^{\lambda} dr^2 - r^2 d\theta^2 - r^2 \sin^2\theta d\phi^2. \quad (3)$$

For an anisotropic NS, the modified Tolman-Oppenheimer-Volkoff (TOV) equations can be obtained by solving Einstein's equations as [23]

$$\frac{dP_r}{dr} = -\frac{(\mathcal{E} + P_r)(m + 4\pi r^3 P_r)}{r(r - 2m)} + \frac{2}{r}(P_t - P_r), \quad (4)$$

$$\frac{dm}{dr} = 4\pi r^2 \mathcal{E}, \quad (5)$$

where the anisotropy parameter is defined as $\sigma = P_t - P_r$. The “ m ” is the enclosed mass corresponding to radius r . Two separate EOSs for P_r and P_t are needed to solve these TOV equations. We consider the EOS for radial pressure $P_r(\mathcal{E})$ from the RMF, SHF, and density-dependent (DD-RMF) models. For transverse pressure (P_t), we take the BL model given in the following [19]:

$$P_t = P_r + \frac{\lambda_{\text{BL}}(\mathcal{E} + 3P_r)(\mathcal{E} + P_r)r^2}{3(1 - 2m/r)}, \quad (6)$$

where the factor λ_{BL} measures the degree of anisotropy in the fluid.

The TOV equations can be solved using the boundary conditions $r = 0, m = 0, P_r = P_c$, and $r = R, m = M$, and $P_r = 0$ for a particular choice of anisotropy. The following conditions which must be satisfied for the anisotropic NS for a perfect fluid are [28,40]

- (1) The pressure and energy density inside the star must be positive, P_r, P_t , and $\mathcal{E} > 0$.
- (2) The gradient of radial pressure and energy density must be monotonically decreasing, $\frac{dP_r}{dr}$, and $\frac{d\mathcal{E}}{dr} < 0$ and maximum value at the center.

- (3) The anisotropic fluid configurations with different conditions such as the null energy ($\mathcal{E} > 0$), the dominant energy ($\mathcal{E} + P_r > 0, \mathcal{E} + P_t > 0$), and the strong energy ($\mathcal{E} + P_r + 2P_t > 0$) must be satisfied inside the star.

- (4) The speed of sound inside the star must obey $0 < c_{s,r}^2 < 1$, and $0 < c_{s,t}^2 < 1$, where $c_s^2 = \frac{\partial P}{\partial \mathcal{E}}$.

- (5) The radial and transverse pressure must be the same at the origin.

We check all the above-mentioned conditions, which are well satisfied in this present case, and some of the results are shown in Figs. 1 and 2 for the IOPB-I parameter set.

The transverse pressure as a function of radius is shown in the upper panel of Fig. 1 for a fixed central density. We observe that the value of P_t increases with increasing λ_{BL} , which supports a more massive NS and vice versa. At the

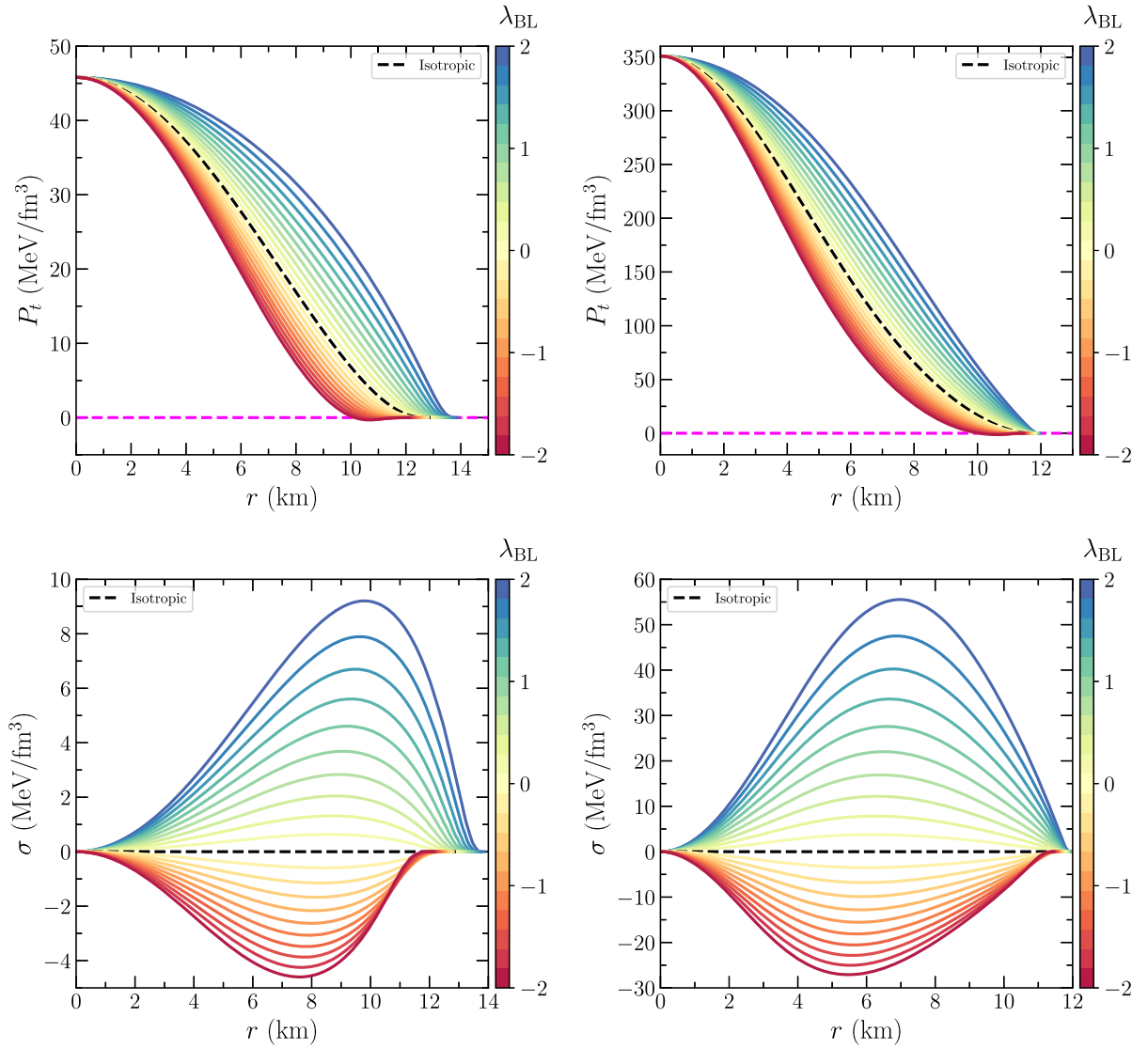


FIG. 1. Upper: the tangential pressure as a function of radius profile of a star with different λ_{BL} both for canonical (left) and maximum mass (right) of the NS corresponds to IOPB-I EOS. The black dashed line is for the isotropic case. Lower: the anisotropy parameter as a function of radius profile.

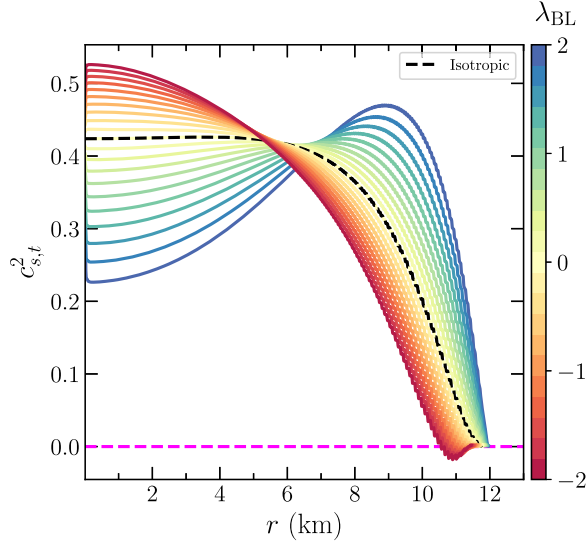


FIG. 2. The speed of sound as a function of radius profile of a star with different λ_{BL} for the maximum mass of the NS corresponds to IOPB-I EOS.

center, both values of P_r and P_t are the same, which satisfies the above-mentioned condition. At the surface part, the positive values of λ_{BL} provide a positive value of P_t and vice versa. This negative value gives the unphysical solutions mainly at the surface part. A more clear picture of the magnitude of the anisotropy parameter can be seen in the lower panel of Fig. 1 for both canonical and maximum mass NS. The magnitude of negativness increases for the maximum star compared to the canonical star.

The speed of sound ($c_{s,t}^2 = \frac{\partial P_t}{\partial \mathcal{E}}$) as a function of radius is depicted in Fig. 2. The $c_{s,t}^2$ satisfies the causality limit in the whole region of the star except at the surface part for the negative λ_{BL} . The transverse pressure and compactness increase with increasing λ_{BL} for a star. In Ref. [35], it has been argued that the black hole limit ($C = 0.5$) is not possible to achieve by increasing the degree of anisotropy with $\lambda_{\text{BL}} = 4.0$ for DDH δ EOS. But at the higher central density, the transverse pressure becomes acausal. We also observed similar results for the IOPB-I EOS with $\lambda_{\text{BL}} > 4.0$.

The mass-radius profiles of the anisotropic NS are solved for IOPB-I EOS for different values of λ_{BL} , which is shown in Fig. 3. The positive values of λ_{BL} increase the maximum masses and their corresponding radii and vice versa. Different observational data such as x-ray, NICER, and GW can constrain the degree of anisotropy inside the NS. Recently, the fastest and heaviest Galactic NS named PSR J0952-0607 in the disk of the Milky Way has been detected to have mass $M = 2.35 \pm 0.17 M_\odot$. We also put this limit to constrain the amount of anisotropy.

The GW190814 event raised a debatable issue: whether the secondary component is the lightest black hole or the heaviest neutron star. Several approaches are already provided in the

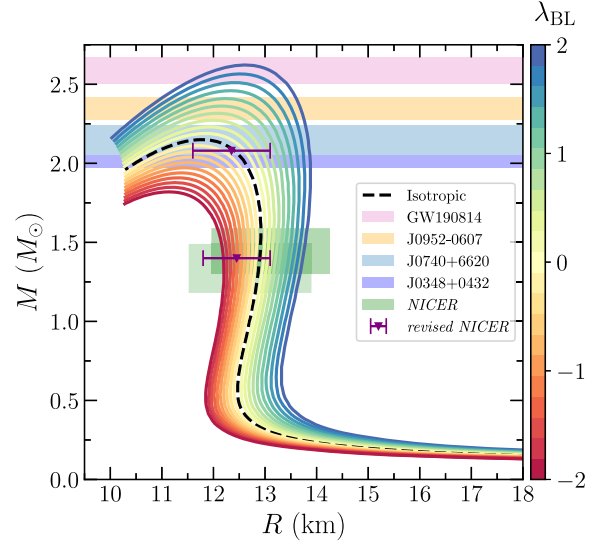


FIG. 3. Mass-radius profiles for anisotropic NS with $-2.0 < \lambda_{\text{BL}} < +2.0$ for IOPB-I EOS. Different color bands signify the masses of the NS observed from the various pulsars, such as PSR J0348 + 0432 [74], PSR J0740 + 6620 [75], heaviest pulsars J0952-0607 [76] and GW190814 [77]. The NICER results are shown with two green boxes from two different analyses [78,79]. The revised NICER results are also shown for the canonical star and $2.08 M_\odot$ (red horizontal error bars) given by Miller *et al.* [80].

literature to explain this behavior [26,81–84]. However, in Ref. [26], they claimed that the secondary component might be an anisotropic NS. Therefore, we put the secondary component mass limit $M = 2.50\text{--}2.67 M_\odot$ in the mass-radius diagram to check whether it reproduced the limit for anisotropy stars within the BL model. We also find that for $\lambda_{\text{BL}} = 1.8\text{--}2$ it reproduces the mass $\sim 2.50\text{--}2.67 M_\odot$ but those values of λ_{BL} do not obey the new NICER constraints [80]. In our case, the $-0.4 < \lambda_{\text{BL}} < +0.4$ almost agrees with the latest observational data.

III. MOMENT OF INERTIA

For a slowly rotating NS, the system's equilibrium position can be obtained by solving Einstein's equation in the Hartle-Thorne metric as [85–87].

$$ds^2 = -e^{2\nu} dt^2 + e^{2\lambda} dr^2 + r^2(d\theta^2 + \sin^2\theta d\phi^2) - 2\omega(r)r^2 \sin^2\theta dt d\phi. \quad (7)$$

The MI of the slowly rotating anisotropic NS was calculated in Ref. [39]:

$$I = \frac{8\pi}{3} \int_0^R \frac{r^5 J \tilde{\omega}}{r - 2M} (\mathcal{E} + P) \left[1 + \frac{\sigma}{\mathcal{E} + P} \right] dr, \quad (8)$$

where $\tilde{\omega} = \bar{\omega}/\Omega$, where $\bar{\omega}$ is the frame dragging angular frequency, $\bar{\omega} = \Omega - \omega(r)$. J is defined as $e^{-\nu}(1 - 2m/r)^{1/2}$.

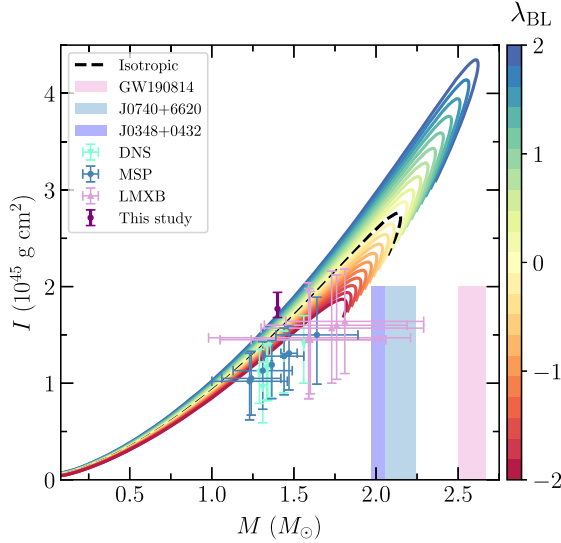


FIG. 4. The moment of inertia of the NS as the function of mass. The error bars are taken from the different pulsar analyses as done in Ref. [88]. We also put the canonical MI, $I_{1.4} = 1.77^{+0.17}_{-0.09} \times 10^{45}$ g cm² obtained in this study for the isotropic star case only.

The $\sigma = P_t - P_r = \frac{\lambda_{\text{BL}} (\mathcal{E} + 3P_r)(\mathcal{E} + P_r)r^2}{3(1 - 2m/r)}$. Hence Eq. (8), can be rewritten using Eq. (6) as

$$I = \frac{8\pi}{3} \int_0^R \frac{r^5 J \tilde{\omega}}{r - 2M} (\mathcal{E} + P) \left[1 + \frac{\lambda_{\text{BL}} (\mathcal{E} + 3P)(\mathcal{E} + P)r^2}{3(\mathcal{E} + P)(1 - 2m/r)} \right] dr. \quad (9)$$

The obtained values of MI for anisotropic NS are shown in Fig. 4 for IOPB-I EOS. The MI of the NS increases with the mass of the NS. Once the stable configuration is achieved, the MI starts to decrease. The anisotropic effects are clearly seen from the figure for different values of λ_{BL} . The error bars represent the MI constraints of the different systems such as double neutron stars (DNS), millisecond pulsars (MSP), and low-mass x-ray binaries (LMXB) inferred by Kumar and Landry [88]. Almost all $I \sim M$ curves satisfy these constraints.

IV. TIDAL DEFORMABILITY

The shape of the NS is deformed when it is present in the external field (ϵ_{ij}) of its companion. Hence, the stars develop the quadrupole moment (Q_{ij}), which is linear dependent on the tidal field and is defined as [89,90]

$$Q_{ij} = -\lambda \epsilon_{ij}, \quad (10)$$

where λ is defined as the tidal deformability of a star. It has relation to the dimensionless tidal Love number k_2 as $\lambda = \frac{2}{3} k_2 R^5$, where R is the radius of the star.

To determine k_2 , we use the linear perturbation in the Throne and Campolattaro metric [91]. We have solved the

Einstein equation and obtained the following second-order differential equation for the anisotropic star [35]:

$$H'' + H' \left[\frac{2}{r} + e^\lambda \left(\frac{2m(r)}{r^2} + 4\pi r(P - \mathcal{E}) \right) \right] + H \left[4\pi e^\lambda \left(4\mathcal{E} + 8P + \frac{\mathcal{E} + P}{dP_t/d\mathcal{E}} (1 + c_s^2) \right) - \frac{6e^\lambda}{r^2} - \nu^2 \right] = 0. \quad (11)$$

The term $dP_t/d\mathcal{E}$ represents the change of P_t [see Eq. (6) for the P_t] with respect to energy density for a fixed value of λ_{BL} .

The internal and external solutions to the perturbed variable H at the star's surface can be matched to get the tidal Love number [89,92]. The value of the tidal Love number can then be calculated using the y_2 , and compactness parameter C is defined as [69,89,90]

$$k_2 = \frac{8}{5} C^5 (1 - 2C)^2 [2(y_2 - 1)C - y_2 + 2] \times \{ 2C[4(y_2 + 1)C^4 + 2(3y_2 - 2)C^3 - 2(11y_2 - 13)C^2 + 3(5y_2 - 8)C - 3(y_2 - 2)] + 3(1 - 2C)^2 \times [2(y_2 - 1)C - y_2 + 2] \log(1 - 2C) \}^{-1}, \quad (12)$$

where y_2 depends on the surface value of H and its derivative

$$y_2 = \frac{rH'}{H} \Big|_R. \quad (13)$$

The gravito-electric Love number (k_2) and its dimensionless tidal deformability ($\Lambda = \lambda/M^5$) are shown in Fig. 5 for the anisotropic NS. Here, we take the positive values of λ_{BL} . This is because the higher negative values predict negative transverse pressure, and the solutions are unphysical, as described in Ref. [35]. The anisotropy effects are rather small for lower negative values of λ_{BL} . Hereafter, we neglect those negative values and take only the positive value of λ_{BL} .

With the increasing value of λ_{BL} , the magnitude of k_2 and its corresponding Λ decrease. The GW170817 event put a limit on the $\Lambda_{1.4} = 190^{+390}_{-120}$, which discarded many older EOSs. In this case, our IOPB-I EOS satisfies both GW170817 and GW190814 limits ($\Lambda_{1.4} = 616^{+273}_{-158}$ under NSBH scenario). For the anisotropic case, all values of λ_{BL} , the predicted $\Lambda_{1.4}$ are almost in the range of the GW170817, and few higher-order values do not lie in the GW190814 limit.

For anisotropic NS, the magnitude of $\Lambda_{1.4}$ is lesser than the isotropic case. Hence, the anisotropic NS tidally deformed less and sustained more time in the inspiral-merger process compared to the isotropic case.

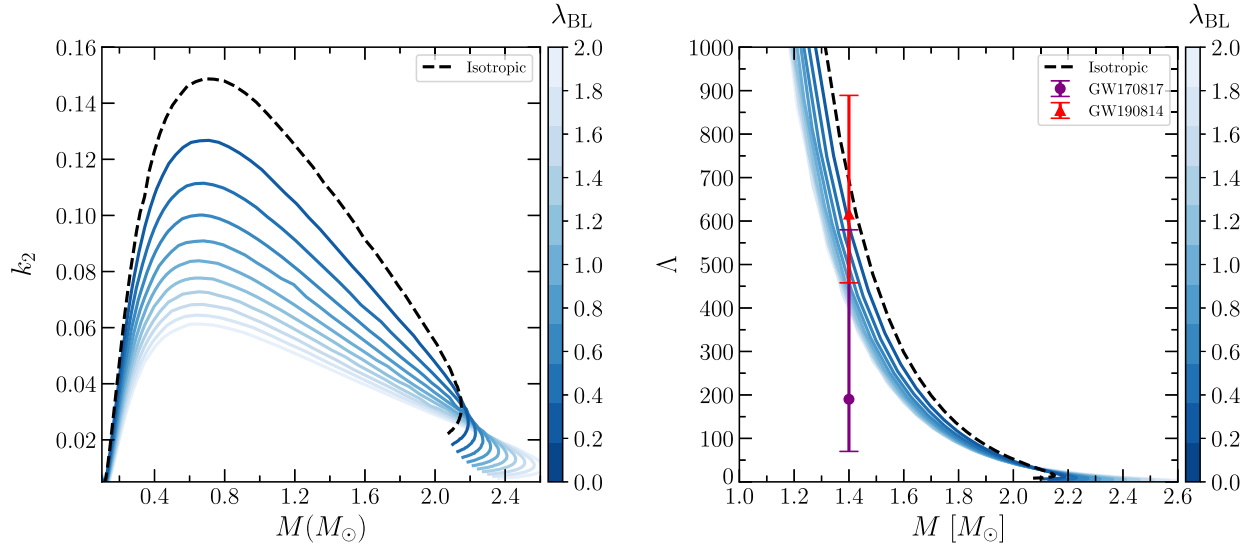


FIG. 5. Left: the tidal Love number as a function of mass for different λ_{BL} corresponds to IOPB-I EOS. Right: the dimensionless tidal deformability as a function of mass for different λ_{BL} corresponds to IOPB-I EOS. The error bars are the observational constraints given by LIGO/Virgo events GW170817 (NS-NS merger) [93] and GW190814 (assuming BH-NS merger) [77].

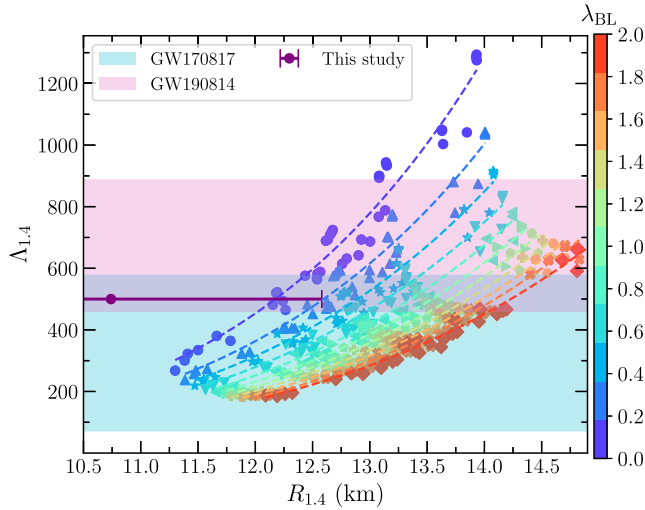


FIG. 6. Relation between $\Lambda_{1,4}$ and $R_{1,4}$ with different anisotropy parameter for different EOSs. The dashed lines are fitted using the function $aR_{1,4}^b$, where a and b are fitting coefficients. We also put the canonical radius limit, $R_{1,4} = 10.74^{+1.84}_{-1.36}$ km, obtained in this study for the isotropic star case only.

In Fig. 6, we show the relation between the canonical dimensionless tidal deformability ($\Lambda_{1,4}$) as a function of canonical radius ($R_{1,4}$) for different values of anisotropy with assumed EOSs. We fit the $\Lambda_{1,4}$ and $R_{1,4}$ with a function $aR_{1,4}^b$ for a fix value of λ_{BL} . The fitting coefficients are given in Table I. In Ref. [94], it is found that the values of a and b are 7.76×10^{-4} and 5.28 respectively with correlation coefficient $r = 0.98$. These coefficients are modified for huge EOS considerations by Annala *et al.* [95]. They found

TABLE I. The fitting coefficients a , and b with relation $\Lambda_{1,4} = aR_{1,4}^b$ corresponding to different λ_{BL} .

λ_{BL}	0.0	1.0	2.0
$a(10^{-5})$	2.28	3.07	3.10
b	6.76	6.37	6.25
r	0.948	0.967	0.973

a robust correlation having $a = 2.88 \times 10^{-6}$ and $b = 7.5$. Malik *et al.* [96] found that the values are 9.11×10^{-5} and 6.13 with 98% correlation.

In this case, we find that $a = 2.28 \times 10^{-5}$ and $b = 6.76$ with correlation coefficients $r = 0.948$ for isotropic NS. With the inclusion of anisotropy, the values of a 's are increasing while b 's are decreasing. Also, we obtained a more robust correlation for anisotropic NS with higher λ_{BL} . For example, for the isotropic case, the value of $r = 0.958$. With increasing λ_{BL} , the correlation coefficients are 0.967, and 0.973 for $\lambda_{\text{BL}} = 1.0$ and 2.0 respectively.

V. UNIVERSAL RELATIONS

Here, we analyze the different types of universal relations among the moment of inertia, tidal deformability, and compactness which are already defined. But, here, we mainly focus on the universal relations for an anisotropic NS. Such approximate universal relations are quite important for astrophysical observations due to the fact that it breaks the degenerates in the data analysis and model selections for different observations such as x-ray, radio, and gravitational waves [42].

A. $I - \Lambda$ relations

The $I - \text{Love}$ relation was calculated by Yagi and Yunes [41] for slowly rotating NS with few EOSs and also included some polytropic EOSs. Later on, these relations were extended by several works to different systems of anisotropic [42–48]. Here, we calculate the $I - \text{Love}$ relations for anisotropic NS.

The MI of the anisotropic NS is calculated using Hartle-Throne approximations. The dimensionless moment of inertia ($\bar{I} = I/M^3$) is plotted as the function of dimensionless tidal deformability (Λ) in Figs. 7–9 with $\lambda_{\text{BL}} = 0-2$ for anisotropic NS. We fit these relations with the formula given in Refs. [88,97],

$$\log_{10} \bar{I} = \sum_{n=0}^4 a_n (\log_{10} \Lambda)^n, \quad (14)$$

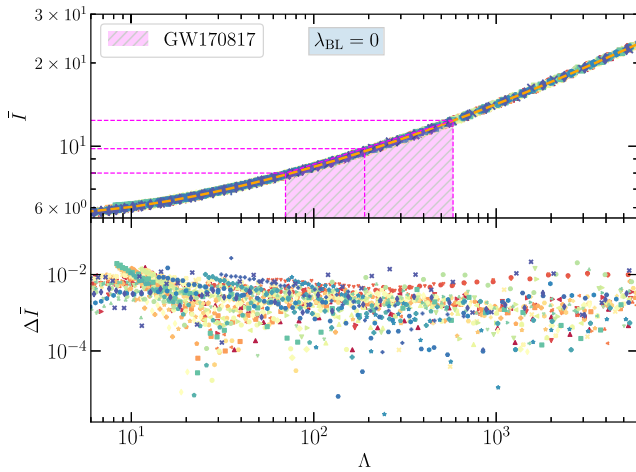


FIG. 7. $\bar{I} - \Lambda$ relation with anisotropy parameter $\lambda_{\text{BL}} = 0$ for assumed EOSs. The orange dashed line is fitted with Eq. (14). The magenta shaded region is canonical tidal deformability data from the GW170817 paper [93]. The lower panel shows the residuals for the fitting calculated using the formula in Eq. (15).

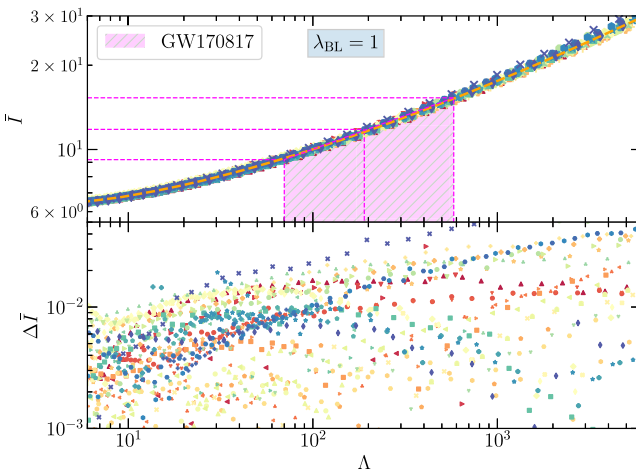


FIG. 8. Same as Fig. 7, but with $\lambda_{\text{BL}} = 1$.

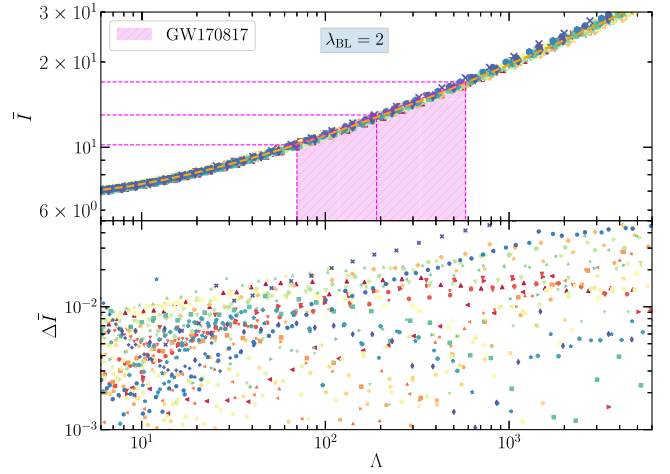


FIG. 9. Same as Fig. 7, but with $\lambda_{\text{BL}} = 2$.

and the coefficients are listed in Table III. Our fit is almost similar with Yagi and Yunes [41] and Landry and Kumar [97]. But the coefficients are slightly modified due to the anisotropy. The residuals are computed with the formula

$$\Delta \bar{I} = \frac{|\bar{I} - \bar{I}_{\text{fit}}|}{\bar{I}_{\text{fit}}}, \quad (15)$$

with reduced chi-squared (χ_r^2) errors and are also enumerated in Table III. With increasing the anisotropy, the value of χ^2 errors increases, which means the EOS insensitive relations get weaker with the addition of anisotropy.

With the help of tidal deformabilities data from the GW170817 and GW190814 events, we put constraints on \bar{I} for isotropic star and found to be $\bar{I}_{1,4} = 14.88^{+1.42}_{-0.76}$, and $21.50^{+1.13}_{-0.91}$ respectively (see Table II). Landry and Kumar [97] obtained the limit as $\bar{I} = 11.10^{+3.64}_{-2.28}$. From the GW170817 event, the value of $\Lambda_{1,4} \leq 800$, which put the upper limit, is found to be $\bar{I} \leq 16.07$ [97]. The theoretical upper limit for the isotropic case almost matches the GW170818 limit. There are many theoretical limits on the MI of the NS [44,49,50,98–102]. The constraints on its value become tighter if we may detect more double pulsars (like PSR J0737-3039) in the near future. For anisotropic cases, the magnitudes for the \bar{I} and I are larger than the

TABLE II. The canonical dimensionless MI ($\bar{I}_{1,4}$), and MI ($I_{1,4} \times 10^{45} \text{gcm}^2$) inferred from GW170817 and GW190814 data.

λ_{BL}	GW170817		GW190814	
	$\bar{I}_{1,4}$	$I_{1,4}$	$\bar{I}_{1,4}$	$I_{1,4}$
0.0	$14.88^{+1.42}_{-0.76}$	$1.77^{+0.17}_{-0.09}$	$21.50^{+1.13}_{-0.91}$	$2.56^{+0.14}_{-0.11}$
1.0	$20.14^{+1.48}_{-0.72}$	$2.40^{+0.17}_{-0.08}$	$30.51^{+1.15}_{-0.90}$	$3.63^{+0.14}_{-0.11}$
2.0	$22.99^{+1.50}_{-0.72}$	$2.74^{+0.18}_{-0.85}$	$35.31^{+1.15}_{-0.89}$	$4.20^{+0.14}_{-0.11}$

TABLE III. The fitting coefficients are listed for $I - \Lambda$, $C - \Lambda$, and $C - I$ relations with $\lambda_{\text{BL}} = 0.0, 1.0, 2.0$. The reduced chi-squared (χ_r^2) is also given for all cases.

$I - \Lambda$				$C - \Lambda$			$C - I$				
$\lambda_{\text{BL}} =$	0.0	1.0	2.0	$\lambda_{\text{BL}} =$	0.0	1.0	2.0	$\lambda_{\text{BL}} =$	0.0	1.0	2.0
$a_0(10^{-1}) =$	7.5026	7.9782	8.3145	$b_0(10^{-1}) =$	3.6873	3.4833	3.4156	$c_0(10^{-2}) =$	5.2024	6.2526	7.3034
$a_1(10^{-2}) =$	4.1857	5.3001	5.6152	$b_1(10^{-2}) =$	-4.1113	-4.0443	-4.0723	$c_1(10^{-1}) =$	-5.1531	-6.0861	-7.0385
$a_2(10^{-2}) =$	8.0495	10.3482	11.1359	$b_2(10^{-3}) =$	1.5301	1.5771	1.6364	$c_2 =$	1.5903	1.87517	2.1721
$a_3(10^{-3}) =$	-8.9478	-15.3418	-18.1670	$b_3(10^{-5}) =$	-1.8874	-2.0472	-2.1929	$c_3 =$	-1.3667	-1.7363	-2.1099
$a_4(10^{-4}) =$	5.4767	10.9879	14.4628	$b_4 =$	$c_4 =$	0.4289	0.6017	0.7684
$\chi_r^2(10^{-5}) =$	0.4133	2.6245	4.5281	$\chi_r^2(10^{-5}) =$	1.0981	0.9022	0.8409	$\chi_r^2(10^{-4}) =$	0.0948	0.8379	4.5028

TABLE IV. The canonical compactness ($C_{1.4}$), and radius ($R_{1.4}$) inferred from GW170817 and GW190814 data.

λ_{BL}	GW170817		GW190814	
	$C_{1.4}$	$R_{1.4}$	$C_{1.4}$	$R_{1.4}$
0.0	$0.192^{+0.03}_{-0.03}$	$10.74^{+1.84}_{-1.36}$	$0.163^{+0.01}_{-0.01}$	$12.69^{+0.71}_{-0.53}$
1.0	$0.177^{+0.03}_{-0.03}$	$11.74^{+2.11}_{-1.54}$	$0.149^{+0.01}_{-0.01}$	$13.94^{+0.80}_{-0.62}$
2.0	$0.169^{+0.03}_{-0.03}$	$12.18^{+2.27}_{-1.65}$	$0.142^{+0.01}_{-0.01}$	$14.58^{+0.88}_{-0.66}$

isotropic case. Because of anisotropy, the mass of the NS increases, which gives rise to the magnitude of MI.

B. $C - \Lambda$ relations

The universal relation for $C - \Lambda$ for the isotropic star was first pointed out by Maselli *et al.* [103]. Later on, it was extended to an anisotropic star by Biswas *et al.* [35] for a few EOSs such as SLy4, APR4, WFF1, DDH δ , and GM1 EOSs. We fit the relation between C and Λ using Eq. (16) for considered EOSs with λ_{BL} which varies from 0 to 2 and the fitting coefficients are listed in Table III. With increasing λ_{BL} , the magnitude of b_n decreases, implying that the fitting is more robust than the isotropic case. The inferred compactness of the isotropic star is more in comparison with the anisotropic star. This signifies that the anisotropic star is less compact than the isotropic one (see Table IV).

We calculate the tidal deformability of the anisotropic NS for the $\lambda_{\text{BL}} = 0, 1, 2$ and shown in Figs. 10–12. We perform the least-squares fit using the approximate formula,

$$C = \sum_{n=0}^3 b_n (\ln \Lambda)^n, \quad (16)$$

where b_n are the coefficients of the fitting given in Table III. The fit residuals are calculated as $\Delta C = |C - C_{\text{fit}}|/C_{\text{fit}}$ and displayed in the lower panel of Fig. 10. We infer the values of both compactness and radius of the canonical star with $\Lambda_{1.4} = 190^{+390}_{-120}$ given by GW170817 [104] and $\Lambda_{1.4} = 616^{+273}_{-158}$ by GW190814 [77] which are enumerated in

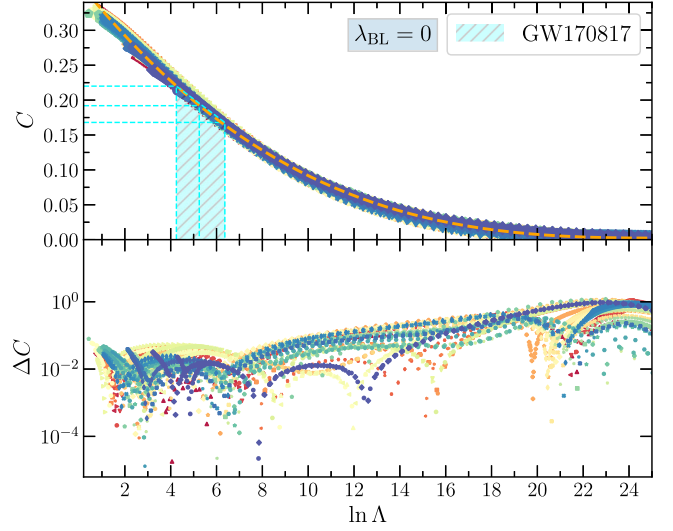


FIG. 10. $C - \Lambda$ relation with anisotropy parameter $\lambda_{\text{BL}} = 0$ for assumed EOSs. The orange dashed line is fitted with Eq. (16). The orange-shaded region is canonical tidal deformability data from the GW170817 paper [93]. The lower panel is the residual of the fitting.

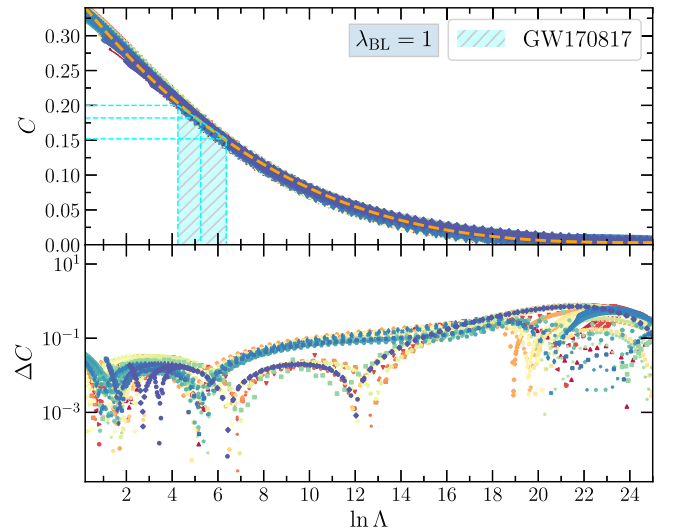


FIG. 11. Same as Fig. 10, but with $\lambda_{\text{BL}} = 1$.

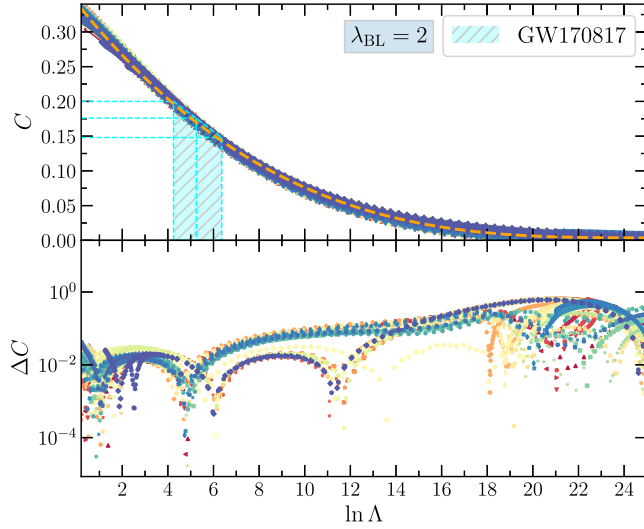


FIG. 12. Same as Fig. 10, but with $\lambda_{\text{BL}} = 2$.

Table IV. Several studies put a limit on the canonical radius of the star with different conditions [88,94,95,105–118]. All the radii constraints are listed in Table 2 of Ref. [116]. Here, we also put the limit on $R_{1.4}$ and $C_{1.4}$ with the help of observational data. It is observed that the highest limit on $R_{1.4}$ is 13.76 km by Fattoyev *et al.* [94] using GW170817 data. If we stick to that limit, then our predictions for $R_{1.4}$ are matched for both isotropic and anisotropic with $\lambda_{\text{BL}} = 1.0$. In case of the lower limit of $R_{1.4}$, the $\lambda_{\text{BL}} = 0.0$ satisfies the limit given by the Tews *et al.* [110] and De *et al.* [114]. Hence, it is observed that the anisotropy inside the NS must be less than 1.0 if one uses the BL model.

C. $C - I$ relations

The dimensionless MI can be expressed as a function of compactness via a lower order polynomial, and it was first pointed out by Ravenhall and Pethick [119]. Later on, several authors have studied and modified the same relations for the double pulsar system with higher-order polynomial fitting [49], scalar-tensor theory and \mathcal{R}^2 gravity [120,121], rotating stars [50], and strange stars [122]. In the present case, we study the $C - I$ relations for anisotropic NS.

Brew and Rezzolla explain the universal behavior of dimensionless MI (I/M^3) which is more accurate than the dimensionless MI defined earlier (I/MR^2). Hence, in this study, we use I/M^3 rather than I/MR^2 . The compactness and dimensionless MI are related in the following polynomial given as [88,97]

$$C = \sum_{n=0}^4 c_n (\log_{10} \bar{I})^{-n}, \quad (17)$$

where c_n is the fitting coefficients and are listed in Table III. The relations between them are depicted in Figs. 13–15 for

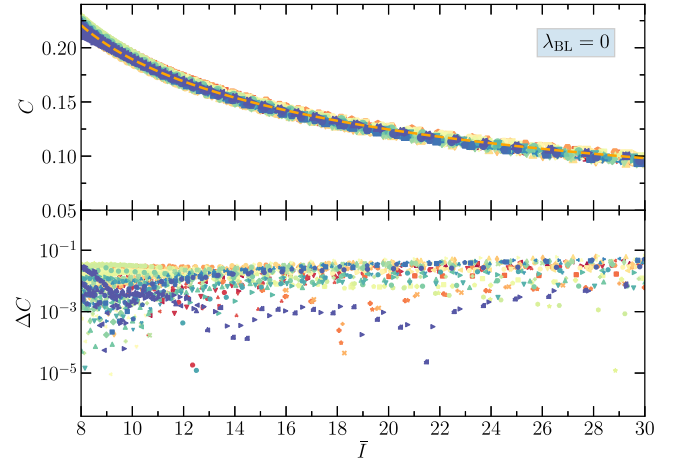


FIG. 13. $C - I$ relation with anisotropy parameter $\lambda_{\text{BL}} = 0$ for assumed EOSs. The orange dashed line is fitted with Eq. (17). The lower panel is the residual of the fitting.

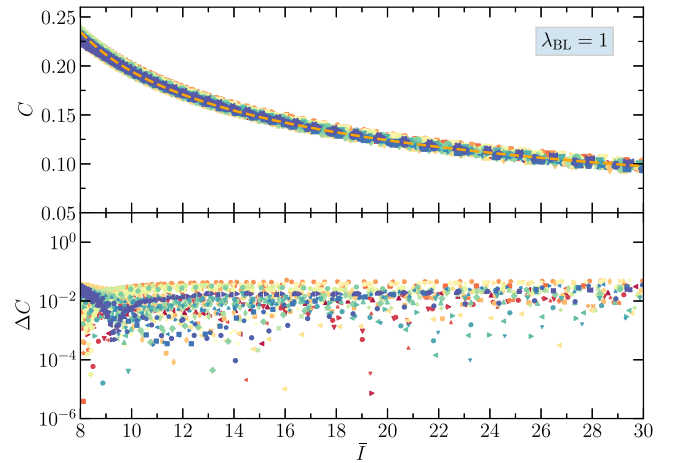


FIG. 14. Same as Fig. 13, but with $\lambda_{\text{BL}} = 1$.

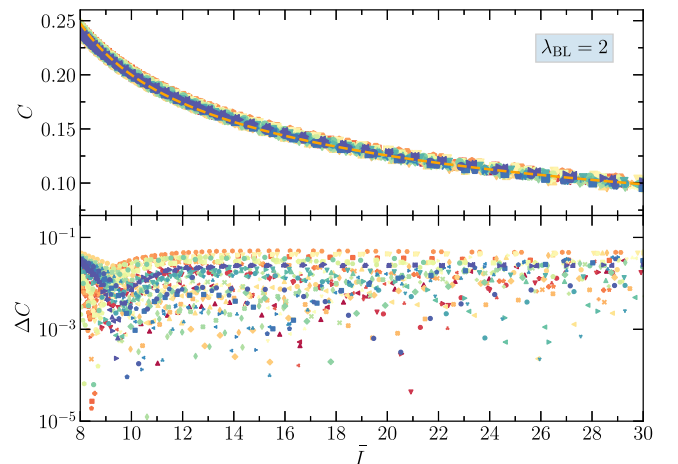


FIG. 15. Same as Fig. 13, but with $\lambda_{\text{BL}} = 2$.

different anisotropy. We can put the constraints on the \bar{I} and C from our previous limit as given in Tables II–IV.

VI. DISCUSSIONS AND CONCLUSION

In this study, we calculate the properties of the anisotropic star based on a simple BL model with 58 parameter sets spanning from relativistic to nonrelativistic cases. The macroscopic property magnitudes such as mass and radius increase due to the anisotropy since an extra contribution comes due to the pressure difference between radial and transverse components. This difference is always model dependent, for example, in the BL and Horvat models. Some of these conditions must be satisfied, such as both transverse and radial pressure, and central energy density must be greater than zero inside the whole star. Extra conditions like null energy, dominant energy, and strong energy are well satisfied inside the whole region of the star. Also, the sound speeds for both components are still valid for the anisotropic stars.

The magnitude of transverse pressure increases by varying λ_{BL} for both canonical and maximum mass stars. But the magnitude is greater for the maximum mass case than for the canonical star. Both transverse pressure and the speed of sound at the surface part become negative, which gives the unphysical solution for higher negative values of anisotropy. Therefore, we do not take such anisotropy cases further in this study. The moment of inertia of the anisotropic star is obtained with a slowly rotating anisotropic star, and it is found that the magnitude increases with anisotropy. Other macroscopic properties, such as tidal Love number and dimensionless tidal deformability, are calculated for the IOPB-I parameter set. We observe that the effects of anisotropy decrease the magnitude of both k_2 and Λ . This implies that the star with higher anisotropy sustains more life in the inspiral-merger phase and vice versa. This is because the star with higher Λ deformed more, the merger process accelerates, and the collapse will happen earlier, as described in Ref. [62]. Hence, one should take the anisotropy inside the NS to theoretically explore the gravitational waves coming from the binary NS inspiral-merger-ringdown phase.

This study calculates the universal relation $I - \text{Love} - C$ for the anisotropic star. The universal relations are mainly required to extract information about the star properties,

which does not become accessible to detect by our detectors/telescopes. The universal relations such as $I - \Lambda$, $C - \Lambda$, and $C - I$ are calculated by changing the anisotropy value. We fit all the relations with a polynomial fit using the least-square method. Our coefficients are almost on par with the different approaches available in the literature. We find that the reduced chi-square errors for $I - \Lambda$, $C - \Lambda$, and $C - I$ are 0.4133×10^{-5} , 1.0981×10^{-5} and 0.0948×10^{-4} respectively for the isotropic star. With anisotropy $\lambda_{\text{BL}} = 1.0$, the errors are 2.6245×10^{-5} , 0.9022×10^{-5} and 0.8379×10^{-4} respectively. The sensitivity of the universal relations such as $I - \Lambda$ and $C - I$ is weaker for the anisotropic star in comparison with the isotropic star. But we obtain the relation between $C - \Lambda$ gets stronger with increasing anisotropy.

We constrain the value of anisotropy using the obtained universal relations from the GW170817 data and find that the value of λ_{BL} is less than 1.0 if one uses the BL model. The canonical radius, compactness, and moment of inertia are found to be $10.74_{-1.36}^{+1.84}$ km, 0.192 ± 0.03 , $14.88_{-0.76}^{+1.42}$ respectively for the isotropic star. For an anisotropic star, the magnitudes of both the canonical radius and the MI increase, but canonical compactness decreases. From the various canonical radius constraints inferred from the GW170817 data, we enumerated the radius of the anisotropic star is less than the $R_{1.4} = 13.85$ km if one uses the BL model. This limit can be modified with different anisotropy models by including phenomena like a magnetic field, quark inside the core, dark matter, etc., in detail. Hence, one can check the different aspects which may produce the anisotropy inside the compact stars and can constrain its degree with the help of observational data.

ACKNOWLEDGMENTS

I would like to thank Professor P. Landry and Professor Bharat Kumar for the discussions on the fitting procedures and would also like to thank Professor A. Sulaksono for formulating the moment of inertia for the anisotropic star. I am extremely thankful to my supervisor Professor S. K. Patra, for the constant support during this project and for carefully reading the manuscript. I also want to thank Ankit Kumar, Jeet Amrit Pattnaik, and Vishal Parmar for the discussions during this project.

-
- [1] J. M. Lattimer and M. Prakash, *Science* **304**, 536 (2004).
 - [2] L. Herrera and N. Santos, *Phys. Rep.* **286**, 53 (1997).
 - [3] S. S. Yazadjiev, *Phys. Rev. D* **85**, 044030 (2012).
 - [4] C. Y. Cardall, M. Prakash, and J. M. Lattimer, *Astrophys. J.* **554**, 322 (2001).

- [5] K. Ioka and M. Sasaki, *Astrophys. J.* **600**, 296 (2004).
- [6] R. Ciolfi, V. Ferrari, and L. Gualtieri, *Mon. Not. R. Astron. Soc.* **406**, 2540 (2010).
- [7] R. Ciolfi and L. Rezzolla, *Mon. Not. R. Astron. Soc.* **435**, L43 (2013).

- [8] J. Frieben and L. Rezzolla, *Mon. Not. R. Astron. Soc.* **427**, 3406 (2012).
- [9] A. G. Pili, N. Bucciantini, and L. Del Zanna, *Mon. Not. R. Astron. Soc.* **439**, 3541 (2014).
- [10] N. Bucciantini, A. G. Pili, and L. Del Zanna, *Mon. Not. R. Astron. Soc.* **447**, 3278 (2015).
- [11] R. F. Sawyer, *Phys. Rev. Lett.* **29**, 382 (1972).
- [12] B. Carter and D. Langlois, *Nucl. Phys.* **B531**, 478 (1998).
- [13] V. Canuto, *Annu. Rev. Astron. Astrophys.* **12**, 167 (1974).
- [14] M. Ruderman, *Annu. Rev. Astron. Astrophys.* **10**, 427 (1972).
- [15] S. Nelmes and B. M. A. G. Piette, *Phys. Rev. D* **85**, 123004 (2012).
- [16] W. A. Kippenhahn Rudolf, *Stellar Structure and Evolution* (Springer, Berlin, 1990), Vol. XVI.
- [17] N. K. Glendenning, *Compact Stars: Nuclear Physics, Particle Physics, and General Relativity* (Springer-Verlag, New York, 1997).
- [18] H. Heiselberg and M. Hjorth-Jensen, *Phys. Rep.* **328**, 237 (2000).
- [19] R. L. Bowers and E. P. T. Liang, *Astrophys. J.* **188**, 657 (1974).
- [20] D. Horvat, S. Ilijić, and A. Marunović, *Classical Quantum Gravity* **28**, 025009 (2010).
- [21] M. Cosenza, L. Herrera, M. Esculpi, and L. Witten, *J. Math. Phys. (N.Y.)* **22**, 118 (1981).
- [22] H. O. Silva, C. F. B. Macedo, E. Berti, and L. C. B. Crispino, *Classical Quantum Gravity* **32**, 145008 (2015).
- [23] D. D. Doneva and S. S. Yazadjiev, *Phys. Rev. D* **85**, 124023 (2012).
- [24] W. Hillebrandt and K. O. Steinmetz, *Astron. Astrophys.* **53**, 283 (1976), <https://ui.adsabs.harvard.edu/abs/1976A&A...53..283H>.
- [25] S. Bayin, *Phys. Rev. D* **26**, 1262 (1982).
- [26] Z. Roupas, *Astrophys. Space Sci.* **366**, 9 (2021).
- [27] D. Deb, B. Mukhopadhyay, and F. Weber, *Astrophys. J.* **922**, 149 (2021).
- [28] G. Estevez-Delgado and J. Estevez-Delgado, *Eur. Phys. J. C* **78**, 673 (2018).
- [29] M. L. Pattersons and A. Sulaksono, *Eur. Phys. J. C* **81**, 698 (2021).
- [30] R. Rizaldy, A. R. Alfarasyi, A. Sulaksono, and T. Sumaryada, *Phys. Rev. C* **100**, 055804 (2019).
- [31] A. Rahmansyah, A. Sulaksono, A. B. Wahidin, and A. M. Setiawan, *Eur. Phys. J. C* **80**, 769 (2020).
- [32] A. Rahmansyah and A. Sulaksono, *Phys. Rev. C* **104**, 065805 (2021).
- [33] L. Herrera, J. Ospino, and A. Di Prisco, *Phys. Rev. D* **77**, 027502 (2008).
- [34] L. Herrera and W. Barreto, *Phys. Rev. D* **88**, 084022 (2013).
- [35] B. Biswas and S. Bose, *Phys. Rev. D* **99**, 104002 (2019).
- [36] S. Das, B. K. Parida, S. Ray, and S. K. Pal, *Phys. Sci. Forum* **2**, 29 (2021).
- [37] Z. Roupas and G. G. L. Nashed, *Eur. Phys. J. C* **80**, 905 (2020).
- [38] A. Sulaksono, *Int. J. Mod. Phys. E* **24**, 1550007 (2015).
- [39] A. Rahmansyah, A. Sulaksono, A. B. Wahidin, and A. M. Setiawan, *Eur. Phys. J. C* **80**, 769 (2020).
- [40] A. M. Setiawan and A. Sulaksono, *Eur. Phys. J. C* **79**, 755 (2019).
- [41] K. Yagi and N. Yunes, *Phys. Rev. D* **88**, 023009 (2013).
- [42] K. Yagi and N. Yunes, *Phys. Rev. D* **91**, 123008 (2015).
- [43] T. Gupta, B. Majumder, K. Yagi, and N. Yunes, *Classical Quantum Gravity* **35**, 025009 (2017).
- [44] J.-L. Jiang, S.-P. Tang, Y.-Z. Wang, Y.-Z. Fan, and D.-M. Wei, *Astrophys. J.* **892**, 55 (2020).
- [45] C.-H. Yeung, L.-M. Lin, N. Andersson, and G. Comer, *Universe* **7**, 111 (2021).
- [46] S. Chakrabarti, T. Delsate, N. Gürlebeck, and J. Steinhoff, *Phys. Rev. Lett.* **112**, 201102 (2014).
- [47] B. Haskell, R. Cioffi, F. Pannarale, and L. Rezzolla, *Mon. Not. R. Astron. Soc.* **438**, L71 (2013).
- [48] D. Bandyopadhyay, S. A. Bhat, P. Char, and D. Chatterjee, *Eur. Phys. J. A* **54**, 26 (2018).
- [49] J. M. Lattimer and B. F. Schutz, *Astrophys. J.* **629**, 979 (2005).
- [50] C. Breu and L. Rezzolla, *Mon. Not. R. Astron. Soc.* **459**, 646 (2016).
- [51] G. A. Lalazissis, J. König, and P. Ring, *Phys. Rev. C* **55**, 540 (1997).
- [52] R. J. Furnstahl, C. E. Price, and G. E. Walker, *Phys. Rev. C* **36**, 2590 (1987).
- [53] R. J. Furnstahl, B. D. Serot, and H.-B. Tang, *Nucl. Phys. A* **615**, 441 (1997).
- [54] R. Furnstahl, B. D. Serot, and H.-B. Tang, *Nucl. Phys. A* **598**, 539 (1996).
- [55] M. Dutra, O. Lourenço, S. S. Avancini, B. V. Carlson, A. Delfino, D. P. Menezes, C. Providência, S. Typel, and J. R. Stone, *Phys. Rev. C* **90**, 055203 (2014).
- [56] S. Typel, *Phys. Rev. C* **71**, 064301 (2005).
- [57] T. H. R. Skyrme, *Philos. Mag. A* **1**, 1043 (1956).
- [58] T. Skyrme, *Nucl. Phys.* **9**, 615 (1958).
- [59] E. Chabanat, P. Bonche, P. Haensel, J. Meyer, and R. Schaeffer, *Nucl. Phys. A* **635**, 231 (1998).
- [60] M. Dutra, O. Lourenço, J. S. Sá Martins, A. Delfino, J. R. Stone, and P. D. Stevenson, *Phys. Rev. C* **85**, 035201 (2012).
- [61] H. C. Das, A. Kumar, B. Kumar, S. K. Biswal, T. Nakatsukasa, A. Li, and S. K. Patra, *Mon. Not. R. Astron. Soc.* **495**, 4893 (2020).
- [62] H. C. Das, A. Kumar, B. Kumar, S. K. Biswal, and S. K. Patra, *J. Cosmol. Astropart. Phys.* **01** (2021) 007.
- [63] H. C. Das, A. Kumar, B. Kumar, and S. K. Patra, *Galaxies* **10**, 14 (2022).
- [64] S. K. Biswal, S. K. Patra, and S.-G. Zhou, *Astrophys. J.* **885**, 25 (2019).
- [65] B. Kumar, S. K. Biswal, and S. K. Patra, *Phys. Rev. C* **95**, 015801 (2017).
- [66] A. Kumar, H. C. Das, S. K. Biswal, B. Kumar, and S. K. Patra, *Eur. Phys. J. C* **80**, 775 (2020).
- [67] B. Kumar, S. Singh, B. Agrawal, and S. Patra, *Nucl. Phys. A* **966**, 197 (2017).
- [68] B. Kumar, S. K. Patra, and B. K. Agrawal, *Phys. Rev. C* **97**, 045806 (2018).
- [69] H. C. Das, A. Kumar, B. Kumar, S. K. Biswal, and S. K. Patra, *Int. J. Mod. Phys. E* **30**, 2150088 (2021).
- [70] O. Lourenço, M. Dutra, C. H. Lenzi, C. V. Flores, and D. P. Menezes, *Phys. Rev. C* **99**, 045202 (2019).
- [71] V. Parmar, H. C. Das, A. Kumar, A. Kumar, M. K. Sharma, P. Arumugam, and S. K. Patra, *Phys. Rev. D* **106**, 023031 (2022).

- [72] M. Fortin, S. S. Avancini, C. Providência, and I. Vidaña, *Phys. Rev. C* **95**, 065803 (2017).
- [73] J. Walecka, *Ann. Phys. (N.Y.)* **83**, 491 (1974).
- [74] J. Antoniadis, P. C. C. Freire, N. Wex, T. M. Tauris, R. S. Lynch *et al.*, *Science* **340**, 1233232 (2013).
- [75] E. Fonseca, H. T. Cromartie, T. T. Pennucci *et al.*, *Astrophys. J. Lett.* **915**, L12 (2021).
- [76] R. W. Romani, D. Kandel, A. V. Filippenko, T. G. Brink, and W. Zheng, *Astrophys. J. Lett.* **934**, L17 (2022).
- [77] R. Abbott, T. D. Abbott, S. Abraham *et al.*, *Astrophys. J.* **896**, L44 (2020).
- [78] M. C. Miller, F. K. Lamb, A. J. Dittmann, S. Bogdanov, Z. Arzoumanian *et al.*, *Astrophys. J.* **887**, L24 (2019).
- [79] T. E. Riley, A. L. Watts, S. Bogdanov, P. S. Ray, R. M. Ludlam *et al.*, *Astrophys. J.* **887**, L21 (2019).
- [80] M. C. Miller, F. K. Lamb, A. J. Dittmann *et al.*, *Astrophys. J. Lett.* **918**, L28 (2021).
- [81] F. J. Fattoyev, C. J. Horowitz, J. Piekarewicz, and B. Reed, *Phys. Rev. C* **102**, 065805 (2020).
- [82] H. C. Das, A. Kumar, and S. K. Patra, *Phys. Rev. D* **104**, 063028 (2021).
- [83] K. Huang, J. Hu, Y. Zhang, and H. Shen, *Astrophys. J.* **904**, 39 (2020).
- [84] Y. Lim, A. Bhattacharya, J. W. Holt, and D. Pati, *Phys. Rev. C* **104**, L032802 (2021).
- [85] J. B. Hartle, *Astrophys. J.* **150**, 1005 (1967).
- [86] J. B. Hartle and K. S. Thorne, *Astrophys. J.* **153**, 807 (1968).
- [87] J. B. Hartle, *Astrophys. Space Sci.* **24**, 385 (1973).
- [88] B. Kumar and P. Landry, *Phys. Rev. D* **99**, 123026 (2019).
- [89] T. Hinderer, *Astrophys. J.* **677**, 1216 (2008).
- [90] T. Hinderer, *Astrophys. J.* **697**, 964 (2009).
- [91] K. S. Thorne and A. Campolattaro, *Astrophys. J.* **149**, 591 (1967).
- [92] T. Damour and A. Nagar, *Phys. Rev. D* **80**, 084035 (2009).
- [93] B. P. Abbott, R. Abbott, T. D. Abbott, F. Acernese, K. Ackley *et al.* (LIGO Scientific and Virgo Collaborations), *Phys. Rev. Lett.* **119**, 161101 (2017).
- [94] F. J. Fattoyev, J. Piekarewicz, and C. J. Horowitz, *Phys. Rev. Lett.* **120**, 172702 (2018).
- [95] E. Annala, T. Gorda, A. Kurkela, and A. Vuorinen, *Phys. Rev. Lett.* **120**, 172703 (2018).
- [96] T. Malik, N. Alam, M. Fortin, C. Providência, B. K. Agrawal, T. K. Jha, Bharat Kumar, and S. K. Patra, *Phys. Rev. C* **98**, 035804 (2018).
- [97] P. Landry and B. Kumar, *Astrophys. J.* **868**, L22 (2018).
- [98] T. Moelndvik and E. Oestgaard, *Nucl. Phys. A* **437**, 239 (1985).
- [99] A. Worley, P. G. Krastev, and B.-A. Li, *Astrophys. J.* **685**, 390 (2008).
- [100] X.-F. Zhao, *Astrophys. Space Sci.* **362**, 95 (2017).
- [101] Y. Lim, J. W. Holt, and R. J. Stahulak, *Phys. Rev. C* **100**, 035802 (2019).
- [102] S. K. Greif, K. Hebeler, J. M. Lattimer, C. J. Pethick, and A. Schwenk, *Astrophys. J.* **901**, 155 (2020).
- [103] A. Maselli, V. Cardoso, V. Ferrari, L. Gualtieri, and P. Pani, *Phys. Rev. D* **88**, 023007 (2013).
- [104] B. P. Abbott, R. Abbott, T. D. Abbott, F. Acernese, K. Ackley *et al.* (The LIGO Scientific and the Virgo Collaborations), *Phys. Rev. Lett.* **121**, 161101 (2018).
- [105] T. Malik, N. Alam, M. Fortin, C. Providência, B. K. Agrawal, T. K. Jha, B. Kumar, and S. K. Patra, *Phys. Rev. C* **98**, 035804 (2018).
- [106] K. Hebeler, J. M. Lattimer, C. J. Pethick, and A. Schwenk, *Phys. Rev. Lett.* **105**, 161102 (2010).
- [107] Y. Lim and J. W. Holt, *Phys. Rev. Lett.* **121**, 062701 (2018).
- [108] E. R. Most, L. R. Weih, L. Rezzolla, and J. Schaffner-Bielich, *Phys. Rev. Lett.* **120**, 261103 (2018).
- [109] O. Lourenço, M. Bhuyan, C. Lenzi, M. Dutra, C. Gonzalez-Boquera, M. Centelles, and X. Viñas, *Phys. Lett. B* **803**, 135306 (2020).
- [110] I. Tews, J. Margueron, and S. Reddy, *Phys. Rev. C* **98**, 045804 (2018).
- [111] N.-B. Zhang, B.-A. Li, and J. Xu, *Astrophys. J.* **859**, 90 (2018).
- [112] T. Dietrich, M. W. Coughlin, P. T. H. Pang, M. Bulla, J. Heinzl, L. Issa, I. Tews, and S. Antier, *Science* **370**, 1450 (2020).
- [113] C. D. Capano, I. Tews, S. M. Brown, B. Margalit, S. De, S. Kumar, D. A. Brown, B. Krishnan, and S. Reddy, *Nat. Astron.* **4**, 625 (2020).
- [114] S. De, D. Finstad, J. M. Lattimer, D. A. Brown, E. Berger, and C. M. Biwer, *Phys. Rev. Lett.* **121**, 091102 (2018).
- [115] S. Köppel, L. Bovard, and L. Rezzolla, *Astrophys. J.* **872**, L16 (2019).
- [116] G. Montaña, L. Tolós, M. Hanauske, and L. Rezzolla, *Phys. Rev. D* **99**, 103009 (2019).
- [117] D. Radice and L. Dai, *Eur. Phys. J. A* **55**, 50 (2019).
- [118] M. W. Coughlin, T. Dietrich, B. Margalit, and B. D. Metzger, *Mon. Not. R. Astron. Soc.* **489**, L91 (2019).
- [119] D. G. Ravenhall and C. J. Pethick, *Astrophys. J.* **424**, 846 (1994).
- [120] K. V. Staykov, D. D. Doneva, and S. S. Yazadjiev, *Phys. Rev. D* **93**, 084010 (2016).
- [121] D. Popchev, K. V. Staykov, D. D. Doneva, and S. S. Yazadjiev, *Eur. Phys. J. C* **79**, 178 (2019).
- [122] M. Bejger and P. Haensel, *Astron. Astrophys.* **396**, 917 (2002).